# Backcalculation of Flexible Pavement Moduli From Dynamic Deflection Basins Using Artificial Neural Networks

ROGER W. MEIER AND GLENN J. RIX

The falling weight deflectometer (FWD) test measures the response of a pavement system to a transient load applied at the pavement surface. A limitation of existing, widely used techniques for backcalculating pavement layer moduli from FWD results is that they are based on a static analysis of pavement response. Previous studies have shown that significant errors in moduli can accrue from the discrepancy between this static assumption and the dynamic nature of the FWD test. Dynamic solutions for pavement response are available, but their computational complexity makes them impractical for use in conventional backcalculation programs that use gradient search or data base techniques. This limitation has been overcome by applying artificial neural network technologies to the backcalculation problem. An artificial neural network has been trained to backcalculate pavement layer moduli for three-layer flexible pavement systems with synthetic dynamic deflection basins. The dynamic pavement response was calculated by using an elastodynamic Green function solution based on a stiffness matrix formulation of the pavement system. The computational efficiency of the trained neural network means that moduli can be backcalculated with a speed that is several orders of magnitude greater than that which can be achieved by conventional gradient search and data base approaches. This is significant because it demonstrates the feasibility of backcalculating pavement layer moduli from dynamic deflection basins in real time.

Falling weight deflectometer (FWD) tests are widely used to assess pavement layer moduli in a nondestructive manner. An FWD test is performed by applying an impulse load to the pavement via a circular plate and measuring the resulting pavement deflections at several radial distances from the plate. The test data are usually summarized as a deflection basin formed from the peak deflections at each measurement location. Pavement layer moduli are then backcalculated from these experimentally determined deflection basins. This is usually accomplished by matching a theoretically calculated deflection basin to the experimental deflections. Most FWD users employ one of two approaches to match deflection basins: (a) a gradient search approach (*1*) in which pavement layer moduli are iteratively adjusted until the theoretical and experimental deflection basins agree within a predefined tolerance and (b) a data base approach (*2*) that uses a combination of pattern searching and interpolation to calculate a theoretical deflection basin from exemplars within a predefined data base of basins.

A limitation of conventional gradient search and data base approaches is that they are based on static deflection basins calculated by using multilayer, linear elastic theory [e.g., WESLEA (*3*)]. The FWD test is inherently a dynamic test because of the impulse-type load applied to the pavement and the resulting inertial forces and resonances within the pavement system. Figure 1 illustrates the difference between static and dynamic deflection basins for a pavement profile with varying depth to bedrock. This pavement profile has a 23-cm (9-in.) asphalt layer over a 30-cm (12-in.) granular base course. The elastic moduli of the asphalt, base, and subgrade are $7 \times 10^6$, $7 \times 10^5$, and $7 \times 10^4$ kPa ($10^6$, $10^5$, and $10^4$ lb/in.$^2$), respectively. Notice that the static deflection basins [Figure 1(*a*)] are strongly influenced by the depth to bedrock, whereas the dynamic deflections [Figure 1(*b*)] are nearly independent of the depth to bedrock. The differences between the static and dynamic displacements can result in significant errors in the backcalculated layer moduli if the backcalculation program uses static deflections (*4–8*).

The computational expense of calculating dynamic deflections hinders their use in backcalculation programs that use either a gradient search or data base approach. Meier and Rix (*9*) proposed the use of artificial neural networks as a fundamentally different approach to backcalculating pavement layer moduli from experimental deflection basins. An artificial neural network is a highly interconnected collection of simple processing elements that can be taught to approximate any continuous functional mapping through repeated exposure to examples of that mapping. Meier and Rix (*9*) trained an artificial neural network to backcalculate pavement layer moduli for a three-layer flexible pavement system using synthetic static deflection basins generated by WESLEA. The trained neural network was able to backcalculate moduli more than 3 orders of magnitude faster than the conventional backcalculation program WESDEF (*1*), which also uses WESLEA. This significant increase in speed makes it possible to backcalculate pavement layer moduli in real time.

In this paper we extend the artificial neural network approach described previously (*9*) to incorporate dynamic deflection basins. The objective is to develop a backcalculation procedure that is based on dynamic deflection basins but that still permits pavement layer moduli to be determined in real time. This is possible because the computational efficiency of the trained neural network is independent of the computational complexity of the algorithms used to create the training data (i.e., the dynamic deflections).

## ARTIFICIAL NEURAL NETWORKS

Artificial neural networks are a computational paradigm completely different from the conventional serial computing introduced by Von Neumann. Instead of the linear sequence of relatively complex tasks

R. W. Meir, Mobility Systems Division, U.S. Army Engineer Waterways Experiment Station Geotechnical Laboratory, 3909 Halls Ferry Road, Vicksburg, Miss. 39180-6199. G. J. Rix, School of Civil and Environmental Engineering, Georgia Institute of Technology, Atlanta, Ga. 30332-0355.

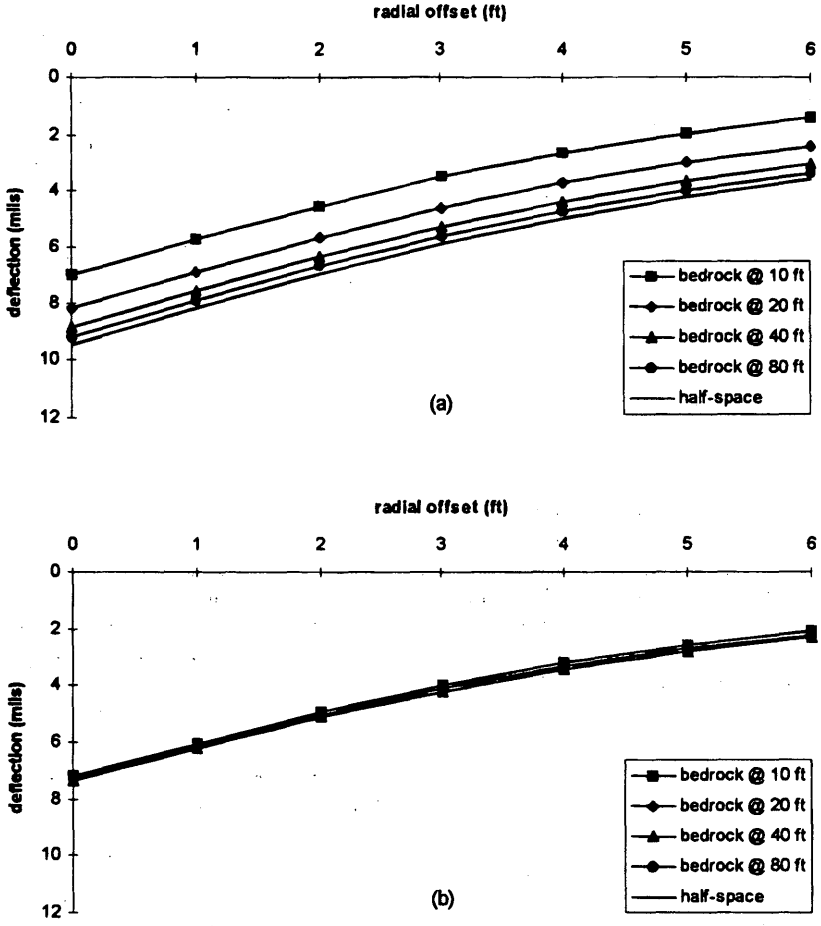


**FIGURE 1 Static (*a*) and dynamic (*b*) deflection basins as a function of depth to bedrock.**

that typifies most algorithmic procedures, artificial neural networks process information in parallel using a large number of operationally simple but highly interconnected processing units. The processing units themselves have certain functional similarities to biological neurons, and their organization bears at least superficial resemblance to the organization of neurons in the brain. This explains the terminology associated with neural computing.

All artificial neural networks are essentially mappers (*10*): for a given input they produce output in accordance with a mapping relationship encoded within their structure. The most common network architecture used for functional mapping (i.e., a unique mapping of real-valued inputs onto real-valued outputs) is the multilayer, feed-forward network. These networks consist of several layers of processing elements (Figure 2). The processing elements pass information, often equated with a signal pattern, from the input layer of the network through a series of hidden layers to the output layer. The signals travel between processing elements along connections whose strengths can be adjusted to amplify or attenuate the signal as it propagates. Each processing element sums the impinging signals to determine a net level of excitation. A nonlinear activation function provides a graded response to that excitation. The element then passes on the response to each of the processing elements in the next layer (Figure 3). The distribution of connection strengths throughout the network uniquely determines the output signal pattern that results from a given input signal pattern. In that respect the connection strengths encode the mapping relationship.

The neural network gains its knowledge through training. A supervised learning method is commonly used to train feed-forward networks. In supervised learning a set of training data (consisting of pairs of input-output patterns exemplifying the mapping to be learned) is presented to the network one example at a time. For each example the input pattern is propagated through the network and the resulting output pattern is compared with the target output. A learning algorithm is used to incrementally adjust the connection weights to reduce the differences between the calculated and the target out-

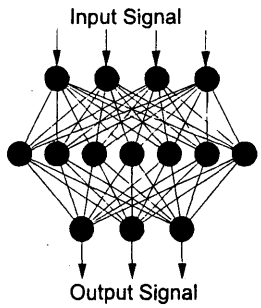


**FIGURE 2 Architecture of a multilayer, feed-forward artificial neural network.**

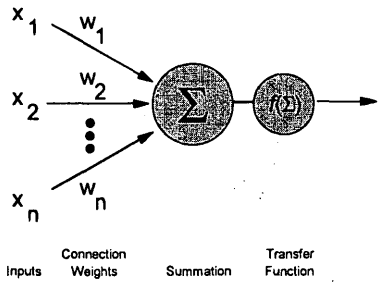


**FIGURE 3 Basic processing element for a multilayer, feed-forward artificial neural network**

puts. This ability to self-adjust is an essential feature of neural computing. It would be impossible to manually establish the connection weights needed to perform any but the simplest of mappings.

Once it is trained the network will provide an approximate functional mapping of any input pattern onto its corresponding output pattern. This process is extremely fast because the input pattern is propagated once through the network, a task that only involves passing weighted sums through the sigmoidal logistic function.

## CALCULATING DYNAMIC PAVEMENT RESPONSE

The best way to train a neural network to map deflection basins onto their corresponding pavement layer moduli would be to use experimentally determined deflection basins along with independently measured pavement layer moduli. Lacking sufficient quantities of such data over a broad range of layer moduli and thicknesses, synthetic deflection basins can be obtained by solving the forward problem with many different combinations of pavement layer properties. A neural network can then be taught to map these synthetic deflection basins back onto their corresponding layer moduli. The latter approach is taken in this paper. This use of synthetic deflection basins to train the artificial neural network is, in principle, analogous to the use of synthetic deflection basins in all conventional basin matching programs. The following sections describe the methodology used to generate the synthetic deflection basins.

### Fourier Superposition Analysis

The dynamic response of a pavement system to the transient loads imposed by the FWD can be analyzed by the principles of Fourier superposition. The first step in Fourier superposition is to decompose the transient loading pulse $p(t)$ into its frequency components, $P(\omega)$, by means of a forward Fourier transform. The next step is to develop a transfer function, $H(\omega)$, that establishes the steady-state response of the pavement system to a unit harmonic excitation at a specified frequency. For the purpose of FWD analysis the appropriate harmonic excitation is a vertical disk load applied at the pavement surface and the required pavement response is the vertical deflection of the pavement surface at some radial distance $r$ from the center of the load. This transfer function is multiplied by the Fourier transform of the applied loads to obtain the response of the pavement in the frequency domain. Finally, the desired pavement deflection history $u(t)$ is obtained by performing an inverse Fourier transform on the calculated frequency-domain response.

The computer implementation of this method requires that the transient loading pulse be discretized into a finite number of applied loads

$$p_j = p(j\Delta t), j = 0, 1, \ldots, N - 1$$

separated by a constant time interval $\Delta t$. These loads can then be transformed into an equivalent number of complex-valued harmonic excitations

$$P_n = P(n\Delta\omega), n = 0, 1, \ldots, (N - 1)/2$$

using a forward fast Fourier transform (FFT) algorithm. These harmonic loads will be separated by a constant frequency interval

$$\Delta\omega = \frac{2\pi}{N\Delta t}$$

where $N$ is the number of points in the discretized loading pulse.

The transfer function is evaluated for each discrete frequency and is multiplied by the appropriate frequency component of the loading pulse to obtain the pavement response in the frequency domain:

$$U_n = H(n\Delta\omega) \times P_n, n = 0, 1, \ldots, N - 1$$

These displacement components are then transformed back into the time domain by using an inverse FFT:

$$u_j = u(j\Delta t), j = 0, 1, \ldots, (N - 1)/2$$

This piecewise-linear deflection history represents the deflection pulse measured in the FWD test.

### Development of Discretized Loading Pulse

The dynamic load imparted to the pavement by the FWD is generated by a free-falling mass hitting a steel plate. A rubber pad beneath the plate uniformly distributes the load to the pavement, and a series of rubber buffers above the plate decelerates the falling mass and conditions the loading pulse. Typical FWD loading pulses for a flexible pavement are illustrated by the light lines in Figure 4.

For programming convenience and computational flexibility a functional analogue to the FWD loading pulse that could be easily varied in both amplitude and duration was desired. Foinquinos et al. (*4*) and Chang et al. (*5*) used a triangular approximation to the loading pulse. Lukanen (*11*) suggests the use of a haversine:

$$p(t) = \frac{P}{2}\left(1 - \cos\frac{2\pi t}{T}\right) \quad (1)$$

where $P$ is the peak amplitude and $T$ is the duration. Both functional approximations were investigated for use in generating synthetic deflection basins.

The four measured loading pulses indicated by the light lines in Figure 4 were normalized to a unit load and were averaged to arrive at a sample FWD loading pulse (indicated by the heavy line in Figure 4). That sample pulse is compared with a triangle and a haversine in both the time and the frequency domains in Figure 5. Both functional analogues were made to have the same duration (26.5 msec) and peak amplitude (1.0) as the average measured pulse.

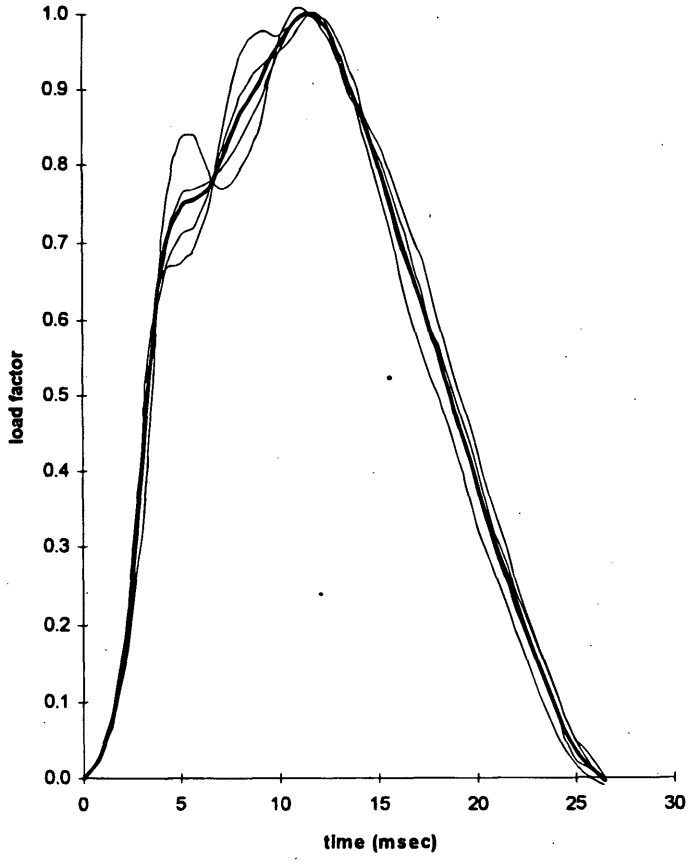


**FIGURE 4 Measured FWD loading pulses and average pulse for four drop heights (*11*).**

Figure 5 shows that the frequency-domain magnitude plots for all three curves are remarkably similar (especially at frequencies below 75 Hz, where all three curves essentially drop to zero) despite the fact that neither of the functional analogues captures the first peak in the time domain. Since all of the calculations in the Fourier superposition analysis occur in the frequency domain, both analogues appear to be suitable surrogates for the measured pulse. Both the triangle and the haversine have slightly lower DC (zero-frequency) values because the total impulse (the area under the force-time curve) is slightly less. The total impulse for the normalized measured pulse is 17.4 msec and the total impulse for the functional analogues is 16.0 msec. To preserve the total energy of the measured FWD pulse, the peak amplitudes of the analogues have to be increased by approximately 9 percent (17.4/16.0 = 1.09).

The haversine was chosen over the triangle for the present study because it better approximates (at least aesthetically) the shape of the sample load pulse and is slightly better behaved in the frequency domain. The perfectly straight sides of the triangular pulse and the sharp discontinuity at its peak result in spurious higher-frequency components that do not exist in the haversine or the measured pulse. Figure 6 compares the measured FWD pulse with an adjusted haversine analogue given by

$$p(t) = 0.545\left(1 - \cos\frac{2\pi t}{26.5}\right) \quad (2)$$

Again, despite the apparent differences in the time domain, there is very close agreement in the frequency domain over the range of 0 to 75 Hz. At frequencies above 75 Hz the magnitudes of both pulses hover near zero, anyway, so any differences are immaterial.

At a frequency of $0.5T^{-1}$, which is equal to 75.47 Hz, the FFT of the haversine pulse has a magnitude identically equal to zero. It would be convenient to use this as a frequency cutoff to limit the bandwidth that must be considered in the Fourier superposition analysis. Because the computational costs incurred in the analysis vary in direct proportion to the number of frequencies that must be analyzed, it was important to either minimize the bandwidth or maximize the frequency interval. To show the feasibility of using a bandwidth-limited analysis, an FFT was performed on the haversine analogue, and all of the components at frequencies higher than 75.47 Hz were set to zero. An inverse FFT was then performed to recover the time-domain loading pulse. The solid line in Figure 7 represents the original haversine, and the symbols show the inverse FFT of the bandwidth-limited function. This shows that little is lost by limiting the bandwidth.

The haversine shown in Figure 7, which was calculated at 32 discrete points in the time domain by using Equation 2, was accepted as the functional analogue of the FWD loading pulse. As a result the Fourier superposition analysis was performed at 31 discrete frequencies. Because the FFT of the haversine load pulse is zero at the

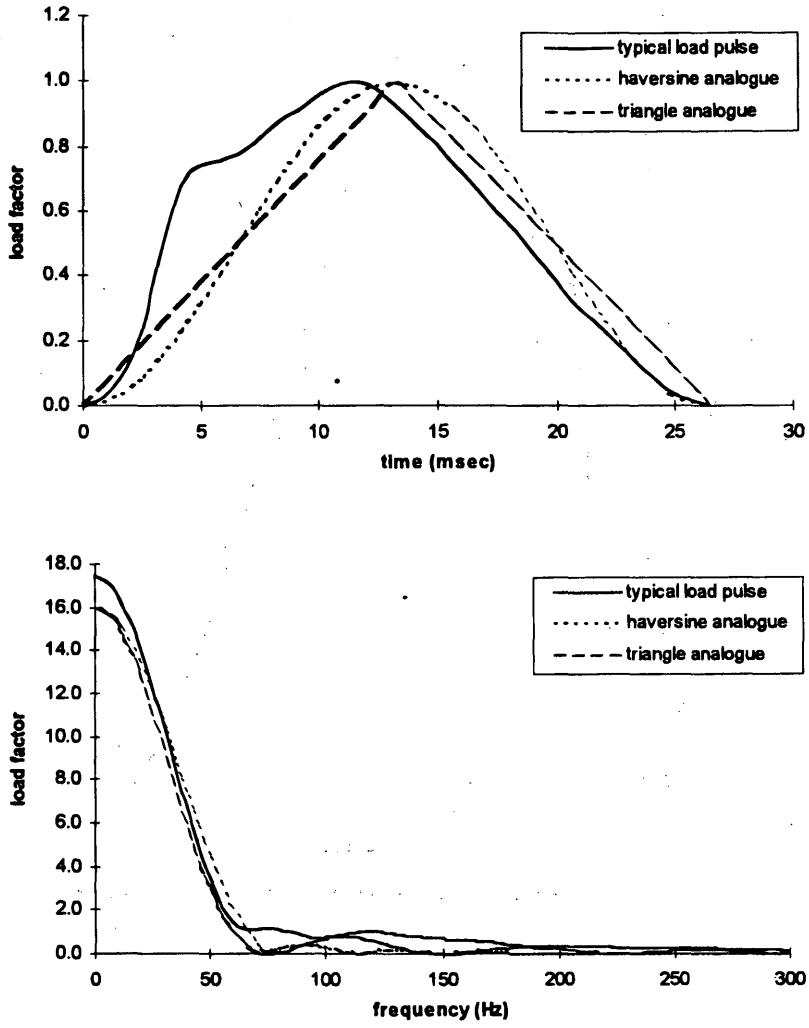


**FIGURE 5 Typical load pulse and functional analogs in time (*a*) and frequency (*b*) domains.**

32nd point (which corresponds to the frequency of 75.47 Hz) there was no need to develop a solution for that frequency.

## Green Function Solution for Transfer Function

The fundamental (Green function) solution for the propagation of waves in layered elastic media was first presented by Thomson (*12*) and was later corrected by Haskell (*13*). Their solution, which has since become known as the Haskell-Thomson formulation, is based on the use of transfer matrices in the frequency-wave number domain that relate the displacements and internal stresses at a given layer interface to those at neighboring layer interfaces. Kausel and Roesset (*14*) developed a complementary solution based on stiffness matrices (analogous to those used in matrix structural analysis) that relate the external loads applied at the layer interfaces to the displacements at the layer interfaces. Those stiffness matrices are a function of both frequency and wave number. Both formulations are, however, computationally inefficient because the matrix elements involve transcendental functions.

Kausel and Peek (*15*) describe a Green function solution based on a discretization (sublayering) of the medium. That solution, described briefly below, is based on the premise that if the sublayer thickness is small relative to the wavelength of interest, it is possible to linearize the transcendental functions and reduce them to algebraic expressions. For most problems the increased efficiency of the algebraic formulation more than compensates for the increased computational requirements of the discretized solution (in which the size of the stiffness matrices increases in direct proportion to the number of sublayers).

Consider a horizontally layered pavement system. The stiffness matrix for each layer is given by the quadratic expression

$$\mathbf{K} = \mathbf{A}k^2 + \mathbf{B}k + \mathbf{G} - \omega^2\mathbf{M} \tag{3}$$

where $k$ is the wave number, $\omega$ is the circular frequency, and the matrices $\mathbf{A}$, $\mathbf{B}$, $\mathbf{G}$, and $\mathbf{M}$, which are given by Kausel and Roesset (*14*), are functions of the material properties $\lambda$ (Lame's constant), $G$ (elastic shear modulus), and $\rho$ (mass density) and the sublayer thicknesses $h$.

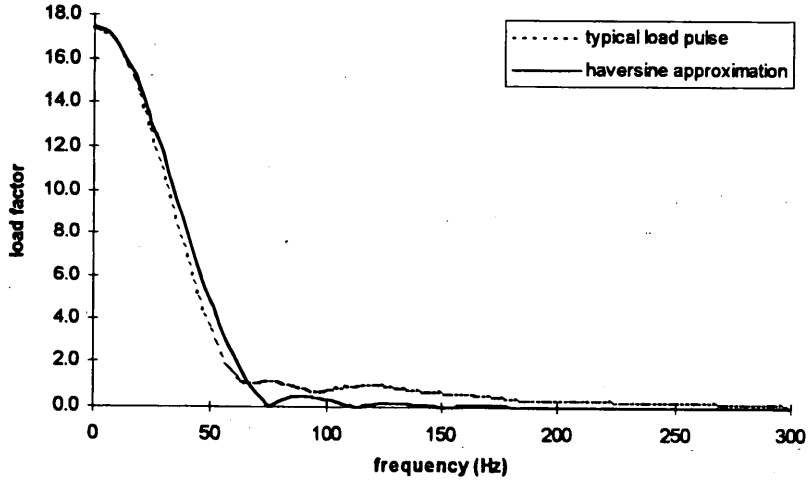


**FIGURE 6 Comparison between typical load pulse and adjusted haversine analogue.**

The global stiffness matrix for the pavement system as a whole is obtained by overlapping the stiffness matrices of the various layers. A numerical expedient suggested by Hull and Kausel (*16*) can be applied at the bottom of the layered system to account for the presence of a half-space instead of rigid rock. The global displacements $\bar{\mathbf{U}}$ can then be related to the global forces $\bar{\mathbf{P}}$ through the assembled global stiffness matrix:

$$\mathbf{K}\bar{\mathbf{U}} = \bar{\mathbf{P}} \tag{4}$$

The natural modes of wave propagation for the layered system are obtained by setting the load vector $\bar{\mathbf{P}}$ equal to zero. This produces the following quadratic eigenvalue problem:

$$(\mathbf{A}k^2 + \mathbf{B}k + \mathbf{G} - \omega^2\mathbf{M})\,\phi = 0 \tag{5}$$

where the eigenvectors $\phi$ are the displacement vectors for each natural mode of propagation. This problem yields $6L$ eigenvalues (modes) $k_j$ with corresponding eigenvectors (mode shapes) $\phi_j$, where $L$ is the total number of sublayers. Only $3L$ of the eigenvectors correspond to waves that propagate away from the applied load. Of those, $2L$ correspond to Rayleigh waves and the remainder correspond to Love waves. Since the latter do not contribute to the vertical deflections produced by a vertical load they can be ignored. Thus, there are really only $2L$ modes of wave propagation of interest here. For those modes of propagation the quadratic eigenvalue problem reduces to a linear problem (albeit with a nonsymmetric characteristic matrix) that can be solved by the inverse power method (*17*). The Green function solution for the vertical surface displacements is expressed in terms of these $2L$ mode shapes:

$$H(\omega) = R\sum_{l=1}^{2L} \phi_w^l \phi_w^l I_{1l} \tag{6}$$

where $R$ is the radius of the vertical disk load, $\phi_w^l$ is the vertical component of the $l$th eigenvector,

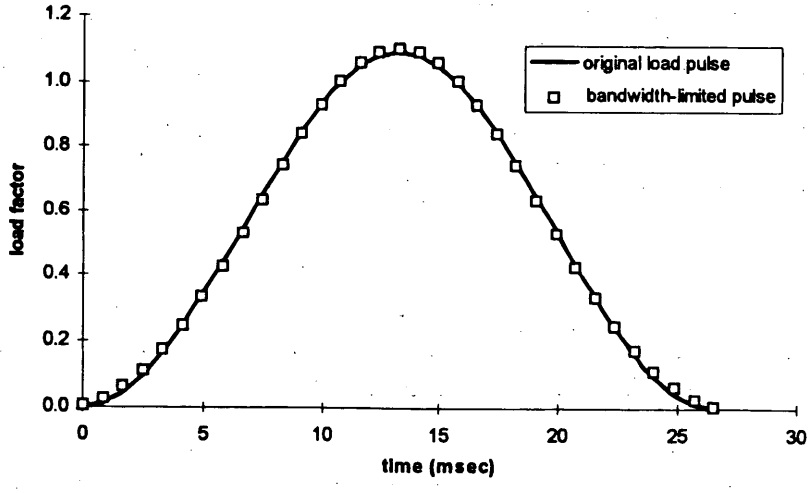


**FIGURE 7 Comparison between original and bandwidth-limited haversine analogues.**

$$I_{1l} = \frac{\pi}{2ik_l} J_0(k_l r)H_1^{(2)}(k_l r) - \frac{1}{Rk_l^2}, \quad \text{for } 0 \le r \le R$$

and

$$I_{1l} = \frac{\pi}{2ik_l} J_1(k_l r)H_0^{(2)}(k_l r), \quad \text{for } r > R$$

The functions $J_0$ and $J_1$ are Bessel functions of the first kind and orders zero and one, respectively. The functions $H_0^{(2)}$ and $H_1^{(2)}$ are Hankel functions of the second kind and orders zero and one, respectively.

### Computer Implementation

Sanchez-Salinero (*18*) implemented the Green function solution described earlier in a FORTRAN computer program. That program was modified to perform the Fourier superposition analysis of the FWD test to obtain the dynamic deflection basins needed to train an artificial neural network. The program performs the following computations for each frequency of analysis:

1. Determine the maximum depth of interest,
2. Discretize the pavement system to the maximum depth of interest,
3. Assemble the global stiffness matrix (Equation 3),
4. Solve the eigenvalue problem (Equation 5) to obtain the propagation modes,
5. Evaluate the transfer function (Equation 6) at each radial distance of interest, and
6. Multiply the results by the FFT of the loading pulse to obtain the deflection components.

For the present study the maximum depth of interest at each frequency was assumed to be twice the length of the Rayleigh waves propagating at that frequency. The global stiffness matrix is assembled by using the half-space approximation of Hull and Kausel (*16*) below that depth. As was shown in Figure 1, the deflection basins obtained from a dynamic analysis of the pavement response are insensitive to bedrock depth for all depths in excess of approximately 3 m (10 ft). As a result the deflection basins produced here will be valid for all but the shallowest depths to bedrock.

Once the global stiffness matrix has been assembled, the eigenvalue problem (Equation 5) is solved by using the inverse power method to obtain the outward-propagating Rayleigh modes. The eigenvalues and their corresponding eigenvectors are used in the solution of the Green function at each radial distance of interest (i.e., each FWD sensor location). These solutions (given by Equation 6) are multiplied by the appropriate frequency component of the loading pulse to obtain the deflection components in the frequency domain. An inverse FFT is then used to recover the deflection pulses in the time domain. Finally, a synthetic deflection basin is assembled from the deflection pulses by finding the peak deflection at each sensor location.

## TRAINING THE ARTIFICIAL NEURAL NETWORK

Backpropagation neural networks are universal approximators, but training times increase rapidly with increasing problem complexity. This places some practical limits on the mappings that can be learned. Instead of trying to train a network to handle a variable number of pavement layers, in the present study the choice was made to train a neural network to backcalculate moduli for a three-layer profile. Each three-layer profile consisted of an asphalt concrete (AC) surface layer, an unstabilized granular base course, and a soil subgrade. The thicknesses and moduli of the AC and base layers and the modulus of the subgrade were randomly selected from uniform distributions within the limits given in Table 1. Because a half-space approximation was used in the Green function solution, the thickness of the subgrade is infinite. Synthetic deflection basins were calculated for a nominal dynamic load of 40 kN (9,000 lb) based on Strategic Highway Research Program-recommended sensor spacings of 0, 20, 30, 45, 60, 90, and 150 cm (0, 8, 12, 18, 24, 36, and 60 in.). For pavement profiles or sensor spacings that differ from these assumed conditions, additional neural networks could easily be trained by the same methodology presented here.

The synthetic deflection basins in the training set are intended to represent deflection basins that would be measured in the field. Typical test specifications for the FWD test (*19*) require a systematic error no greater than 2 percent of the measured deflection and a repeatability error no greater than 2 μm (0.08 mils). As illustrated in a previous study (*20*), these potential inaccuracies can be accommodated by introducing random noise during training, a technique known as noise injection. The random noise was added to each of the seven deflections in each training example just before presenting it to the network. In this way, even though the training basins were constantly reused, the added noise was different every time. The random variates were drawn from uniform distributions whose limits were equal to the larger of ±2 percent of the ideal deflection or ±2.5 μm (±0.1 mils). The latter was made slightly larger than the test specification to permit some room for error.

The study used the same network architecture used previously (*9*) for mapping static deflection basins with noise injection. Despite the increased fidelity of the model used to create the training data, both networks map nine-element vectors of pavement deflections and layer thicknesses onto three-element vectors of pavement moduli. Since this complexity of the mapping task is essentially the same, the same network architecture, which uses two hidden layers with 15 neurons apiece, should suffice.

**TABLE 1 Pavement Layer Properties Used To Train the Neural Networks**

| Layer | Layer Modulus (MPa)[a] | Layer Thickness (cm)[b] | Poisson's Ratio |
|---|---|---|---|
| Asphalt | 1725 - 20,685 | 5 - 30 | 0.325 |
| Base | 35 - 1035 | 15 - 75 | 0.35 |
| Subgrade | 35 - 345 | 3050 | 0.35 |

[a] 1 MPa = 0.145 ksi
[b] 1 cm = 0.394 in

Network training proceeded by iteratively presenting the training examples to the network. Each pass through the set of 10,000 examples constituted a training "epoch." During each epoch the first 9,750 examples were used to train the network. The remaining 250 examples were set aside to test the network at the conclusion of training. (Neural networks should never be tested with the same data that were used to train them. It is important that the network be able to generalize beyond the training examples instead of simply memorizing them.) At first the mean squared output error drops rapidly as the training epochs are completed [Figure 8(*a*)]. With further training the output error asymptotically approaches some minimum level. Network training continued until it was clear that the computational expense of continued training outweighed any further increases in network accuracy.

At the conclusion of training the 250 deflection basins previously set aside were used to check the accuracy of the network. As with the other 9,750 deflection basins, random noise was added to these test basins to better simulate real measurements. Tests to determine the repeatability of FWD measurements (*21*) have shown that individual transducers have a standard deviation of ±1.95 μm. Because this error is random, it can be lessened by replicating the test and averaging the results. Irwin et al. (*21*) recommend that three to five replicates be conducted for each test. The amount of noise added to each deflection was therefore established by averaging five random variates drawn from a Gaussian distribution with a mean of zero and a standard deviation that was rounded off to ±2 μm (0.08 mils). Because these random variates were drawn from a Gaussian distribution instead of the uniform distribution used to train the network, it is possible that some of these test basins contained more noise than was present in the training set.

Figures 8(*b*), 8(*c*), and 8(*d*) compare the target and computed moduli for the asphalt, base, and subgrade layers, respectively, for the 250 test basins. The neural network clearly learned the mapping from deflection basins to subgrade moduli extremely well, despite the presence of noise. It also learned the mapping from deflection basins to asphalt moduli very well, although there was a slight tendency toward underestimation for the stiffer pavements. Considering that the base moduli are always the hardest to backcalculate, the network has done a very good job with those, too. Figure 9(*a*) shows that the base modulus error is less than 15 percent for more than 80 percent of the pavement profiles. Figures 9(*b*), 9(*c*), and 9(*d*) collectively show that the 20 percent of the profiles with the greatest

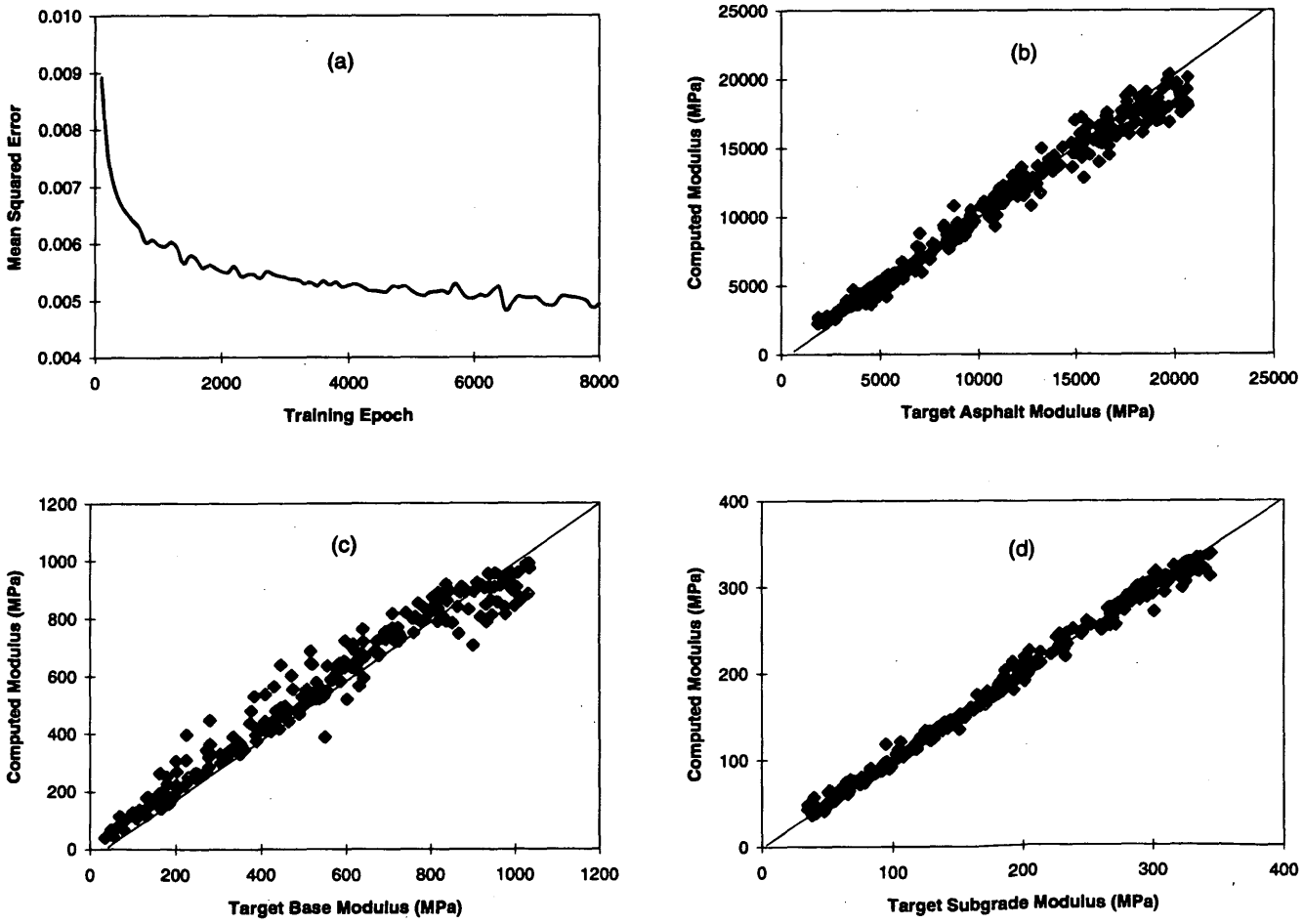


**FIGURE 8 Training progress (*a*) and testing results for asphalt (*b*), base (*c*), and subgrade (*d*) moduli.**

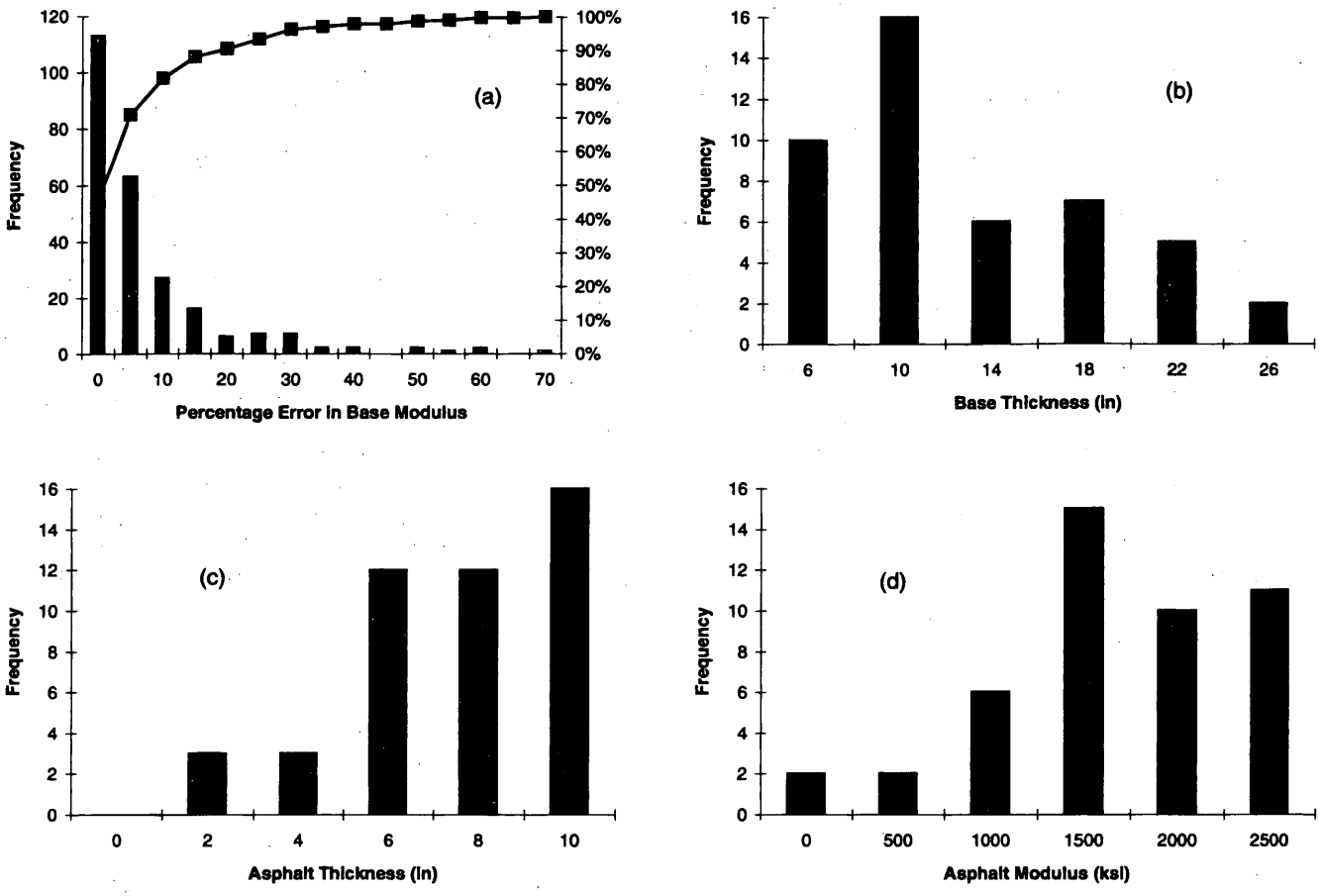


**FIGURE 9 Error distribution and pavement layer property distributions for 80th percentile errors.**

base modulus error tend to have a relatively rigid (thin, stiff or both) asphalt layer and a relatively thin base course. The rigidity of the surface layer makes the thin base layer essentially invisible, a problem inherent to the FWD test itself.

## SUMMARY AND CONCLUSIONS

A previous study (*9*) showed that an artificial neural network could be trained to backcalculate pavement layer moduli from FWD deflection basins. That study used synthetic deflection basins calculated by using a static analysis of pavement response. In the present study an artificial neural network was successfully trained to backcalculate pavement layer moduli from synthetic deflection basins calculated by using a dynamic analysis of pavement response based on Green functions. Because the FWD test is inherently dynamic, these dynamic deflection basins are a significantly better analogue for the experimental results that would be obtained in the field.

Because the computational efficiency of the trained neural network is independent of the computational complexity of the algorithms used to create the training data, this neural network takes no longer to run than those in the previous study, and it still runs in real time. The authors know of no other method for backcalculating pavement layer moduli from dynamic deflection basins in real time.

## ACKNOWLEDGMENTS

The information presented herein, unless otherwise noted, was obtained from research conducted by the U.S. Army Engineer Waterways Experiment Station. The authors acknowledge the advice and support provided throughout the study by Albert J. Bush III and Don R. Alexander of the Waterways Experiment Station. The authors acknowledge the assistance and encouragement provided by José M. Roesset of the University of Texas at Austin and Eduardo Kausel of the Massachusetts Institute of Technology.

## REFERENCES

1. Bush, A. J., III. *Nondestructive Testing for Light Aircraft Pavements, Phase II: Development of the Nondestructive Testing Methodology*. Report FAA-RD-80-9-II. FAA, U.S. Department of Transportation, 1980.
2. Uzan, J., R. L. Lytton, and F. P. Germann. General Procedure for Backcalculating Layer Moduli. In *Nondestructive Testing of Pavements and Backcalculation of Moduli* (A. J. Bush III and G. Y. Baladi, eds.). ASTM 1026. ASTM, Philadelphia, 1989, pp. 217–228.

3. Van Cauwelaert, F. J., D. R. Alexander, T. D. White, and W. R. Barker. Multilayer Elastic Program for Backcalculating Layer Moduli in Pavement Evaluation. In *Nondestructive Testing of Pavements and Backcalculation of Moduli* (A. J. Bush III and G. Y. Baladi, eds.). ASTM 1026. ASTM, Philadelphia, 1989, pp. 171–188.
4. Foinquinos, R., J. M. Roesset, and K. H. Stokoe II. Response of Pavement Systems to Dynamic Loads Imposed by Nondestructive Tests. Presented at 73rd Annual Meeting of the Transportation Research Board, Washington, D.C., 1993.
5. Chang, D. W., V. Y. Kang, J. M. Roesset, and K. H. Stokoe II. Effect of Depth to Bedrock on Deflection Basins Obtained with Dynaflect and FWD Tests. In *Transportation Research Record 1355*, TRB, National Research Council, Washington, D.C., 1990, pp. 8–16.
6. Davies, T. G., and M. S. Mamlouk. Theoretical Response of Multilayer Pavement Systems to Dynamic Nondestructive Testing. In *Transportation Research Record 1022*, TRB, National Research Council, Washington, D.C., 1985, pp. 1–7.
7. Shao, K.-Y., J. M. Roesset, and K. H. Stokoe II. *Dynamic Interpretation of Dynaflect and Falling Weight Deflectometer Tests on Pavement Systems*. Research Report 437-1. Center for Transportation Research, University of Texas at Austin, Aug. 1986.
8. Ketchum, S. A. Dynamic Response Measurements and Identification Analysis of a Pavement During Falling Weight Deflectometer Experiments. In *Transportation Research Record 1415*, TRB, National Research Council, Washington, D.C., 1993, pp. 78–87.
9. Meier, R. W., and G. J. Rix. Backcalculation of Flexible Pavement Moduli Using Artificial Neural Networks. Presented at 73rd Annual Meeting of the Transportation Research Board, Washington, D.C., 1993.
10. Wasserman, P. D. *Advanced Methods in Neural Computing*. Van Nostrand Reinhold, New York, 1993.
11. Lukanen, E. O. Effects of Buffers on Falling Weight Deflectometer Loadings and Deflections. In *Transportation Research Record 1355*, TRB, National Research Council, Washington, D.C., 1993, pp. 37–51.
12. Thomson, W. T. Transmission of Elastic Waves Through a Stratified Soil Medium. *Journal of Applied Physics*, Vol. 21, No. 1, Feb. 1950, pp. 89–93.
13. Haskell, N. A. The Dispersion of Surface Waves on Multilayered Media. *Bulletin of the Seismological Society of America*, Vol. 43, No. 1, Feb. 1953, pp. 17–34.
14. Kausel, E., and J. M. Roesset. Stiffness Matrices for Layered Soils. *Bulletin of the Seismological Society of America*, Vol. 71, No. 6, Dec. 1981, pp. 1743–1761.
15. Kausel, E., and R. Peek. Dynamic Loads in the Interior of a Layered Stratum: An Explicit Solution. *Bulletin of the Seismological Society of America*, Vol. 72, No. 5, October 1982, pp. 1459–1481.
16. Hull, S. W., and E. Kausel. Dynamic Loads in Layered Half-Spaces. *Proc., Fifth Engineering Mechanics Division Specialty Conference*, Laramie, Wyo., New York, ASCE, 1984.
17. Young, D. M., and R. T. Todd. *A Survey of Numerical Mathematics*, Vol. II. Dover Publications, Inc., New York, 1973, pp. 918–920.
18. Sanchez-Salinero, I. *Analytical Investigation of Seismic Methods Used for Engineering Applications*. Ph.D. thesis, University of Texas at Austin, May 1987.
19. Standard Test Method for Deflections with a Falling-Weight-Type Impulse Load Device. In *Annual Book of ASTM Standards*, Vol. 04.03, ASTM, Philadelphia, 1993, pp. 566–568.
20. Matsuoka, K. Noise Injection into Inputs in Back-Propagation Learning. *IEEE Transactions on Systems, Man, and Cybernetics*, Vol. 22, No. 3, 1992, pp. 436–440.
21. Irwin, L., W. Yang, and R. Stubstad. Deflection Reading Accuracy and Layer Thickness Accuracy in Backcalculation of Pavement Layer Moduli. In *Nondestructive Testing of Pavements and Backcalculation of Moduli* (A. J. Bush III and G. Y. Baladi, eds.). ASTM 1026. ASTM, Philadelphia, 1989, pp. 229–244.

---

*The views of the authors do not purport to reflect the position of the Department of the Army or the U.S. Department of Defense.*

*Publication of this paper sponsored by Committee on Strength and Deformation Characteristics of Pavement Sections.*